Inorg. Chem. **2005**, *44*, 3203–3209

Nanophase Iron Phosphate, Iron Arsenate, Iron Vanadate, and Iron Molybdate Minerals Synthesized within the Protein Cage of Ferritin

Jup Polanams, Alisha D. Ray, and Richard K. Watt*

Department of Chemistry, University of New Mexico, Albuquerque, New Mexico 87131-0001

Received August 25, 2004

Nanoparticles of iron phosphate, iron arsenate, iron molybdate, and iron vanadate were synthesized within the 8 nm interior of ferritin. The synthesis involved reacting Fe(II) with ferritin in a buffered solution at pH 7.4 in the presence of phosphate, arsenate, vanadate, or molybdate. O_2 was used as the oxidant to deposit the Fe(III) mineral inside ferritin. The rate of iron incorporation into ferritin was stimulated when oxo-anions were present. The simultaneous deposition of both iron and the oxo-anion was confirmed by elemental analysis and energy-dispersive X-ray analysis. The ferritin samples containing iron and one of the oxo-anions possessed different UV/vis spectra depending on the anion used during mineral formation. TEM analysis showed mineral cores with ~8 nm mineral particles consistent with the formation of mineral phases inside ferritin.

Introduction

The ferritin protein functions in biological systems to sequester and store excess iron. These iron reserves can be accessed when the organism is exposed to iron-limiting growth conditions.[1] Ferritin is composed of 24 similar subunits that interact to form a spherical protein complex with a hollow interior.[2] The protein shell functions as an insulator to protect other cellular components from biologically dangerous reactions catalyzed by iron. The iron enters and leaves the ferritin protein through channels that form at subunit interfaces or through pores in the folds of the individual protein subunits.[2,3] The interior cavity of ferritin is ~8 nm in diameter and has an interior volume that can store up to 4500 iron atoms as an iron oxide−hydroxide mineral.[2] Along with iron, ferritin also accumulates phosphate within the ferritin mineral core.[4,5] The phosphate content associated with the iron mineral core differs depending on the type of cells used as the source of the ferritin. As isolated, mammalian ferritin contains approximately 10 iron atoms/phosphate group,[6] whereas the phosphate content of plant[7] and bacterial ferritin[8−12] is much higher with an iron-to-phosphate ratio approaching a 1:1 ratio in bacterial ferritin. In mammalian ferritin, phosphate appears to be primarily bound on the iron mineral surface and has been shown to provide binding sites for incoming iron atoms.[5,8,13] Another role for phosphate is to catalyze the oxidation of Fe^{2+} ions on the mineral core surface of ferritin.[14]

The ~8 nm diameter cavity of ferritin and the ability to bind large numbers of iron atoms make ferritin a target of study for encapsulating alternate metal minerals into ferritin for nanomaterial applications (see below). Furthermore, ferritin possesses other properties that make it useful for the synthesis of materials. Ferritin is stable over a large pH range

* Author to whom correspondence should be addressed. E-mail: rwatt@unm.edu. Tel.: 1-505-277-5328. Fax: 1-505-277-2609.

(1) Abdul-Tehrani, H.; Hudson, A. J.; Chang, Y. S.; Timms, A. R.; Hawkins, C.; Williams, J. M.; Harrison, P. M.; Guest, J. R.; Andrews, S. C. *J. Bacteriol.* **1999**, *181*, 1415−1428.
(2) Harrison, P. M.; Hempstead, P. D.; Artymiuk, P. J.; Andrews, S. C. Structure−Function Relationships in the Ferritins. In *Metal Ions in Biological Systems*; Marcel Dekker: New York, NY 10016, 1998; Vol 35, pp 435−477.
(3) Douglas, T.; Ripoll, D. R. *Protein Sci.* **1998**, *7*, 1083−1091.
(4) Granick, S.; Hahn, P. F. *J. Biol. Chem.* **1944**, *155*, 661−669.
(5) Treffry, A.; Harrison, P. M. *Biochem. J.* **1978**, *171*, 313−320.
(6) Michaelis, L.; Coryell, C. D.; Granick, S. *J. Biol. Chem.* **1943**, *28*, 329−336.
(7) Wade, V. J.; Treffry, A.; Laulhere, J. P.; Bauminger, E. R.; Cleton, M. I.; Mann, S.; Briat, J. F.; Harrison, P. M. *Biochim. Biophys. Acta* **1993**, *1161*, 91−96.
(8) Rohrer, J. S.; Islam, Q. T.; Watt, G. D.; Sayers, D. E.; Theil, E. C. *Biochemistry* **1990**, *29*, 259−264.
(9) Bauminger, E. R.; Cohen, S. G.; Dickson, D. P. E.; Levy, A.; Ofer, S.; Yariv, J. *Biochim. Biophys. Acta* **1980**, *623*, 237−242.
(10) Mann, S.; Bannister, J. V.; Williams, R. J. P. *J. Mol. Biol.* **1986**, *188*, 225−232.
(11) Treffry, A.; Harrison, P. M.; Cleton, M. I.; Debruijn, W. C.; Mann, S. *J. Inorg. Biochem.* **1987**, *31*, 1−6.
(12) Watt, G. D.; Frankel, R. B.; Jacobs, D.; Huang, H. Q. *Biochemistry* **1992**, *31*, 5672−5679.
(13) Huang, H. Q.; Watt, R. K.; Frankel, R. B.; Watt, G. D. *Biochemistry* **1993**, *32*, 1681−1687.
(14) Johnson, J. L.; Cannon, M.; Watt, R. K.; Frankel, R. B.; Watt, G. D. *Biochemistry* **1999**, *38*, 6706−6713.

10.1021/ic048819r CCC: $30.25
Published on Web 03/26/2005

(2−10) and is stable at temperatures up to 70 °C.[15] Ferritin forms 2-dimensional crystals on surfaces forming ordered patterns.[16] The ordered arrangement of ferritin molecules leads to the concomitant deposition of the metal cores in an ordered 2-dimensional array. High temperatures (400−500 °C) can be used to pyrolize the protein shell leaving the metal core deposited on the indicated substrates. These properties of ferritin can be used to template the ferritin protein in ordered arrays to align metal particles for materials applications.

Previous efforts to prepare ferritin samples substituted with nonnative metal cores have been successful. These synthetic procedures include the preparation of ferritins containing cobalt,[15,17] manganese,[18] iron sulfide,[19] cadmium sulfide,[20] uranium,[21,22] cobalt and platinum,[23−25] nickel,[26] chromium,[26] and magnetite.[20] Uses for ferritin with such synthetic cores include medical imaging, radiopharmaceuticals, quantum dots and nanobatteries, photocatalysts, and magnetic memory devices.

The goals of the present work were 2-fold. The entry pathway for phosphate into ferritin is unknown; therefore, the first goal was to design experiments that might provide insight about the process of phosphate entry into ferritin. The second goal was to determine if phosphate analogues could be incorporated into ferritin. The second goal, if successful, will provide a new synthetic method for preparing iron/oxo-anion nanomaterials in ferritin. The catalytic properties of bulk iron/oxo-anion complexes of iron phosphate, iron vanadate, and iron molybdate have been documented.[27−31] The synthesis of these iron/oxo-anion complexes in ferritin, followed by depositing ferritin arrays on silica, gold, or other surfaces, can be used to prepare and template nanocatalysts of these materials. This paper reports the successful synthesis and initial characterization of iron arsenate, iron vanadate, and iron molybdate cores inside the ferritin protein.

Experimental Section

Iron Incorporation. Apo-horse spleen ferritin was purchased from Sigma. Ferritin samples were reconstituted with iron or were reconstituted with iron in the presence of one of the oxo-anions, phosphate, arsenate, vanadate, or molybdate, using the following procedure. An apo-ferritin solution (0.25 μM, 2.5 mL) was prepared in 0.1 M Mops buffer pH 7.4, 0.05 M NaCl. The indicated oxo-anion (phosphate, arsenate, vanadate, or molybdate) was added to the apo-ferritin solution for a final oxo-anion concentration of 1.0 mM. This solution was stirred aerobically in a cuvette in an Ocean Optics Chem 2000 UV/vis spectrophotometer, and Fe^{2+} ions were added from either a 0.010 M $FeSO_4$ or 0.010 M $FeCl_2$ stock solution to a final concentration of 50 μM (~200 Fe^{2+}/ferritin). The iron loading into ferritin was monitored spectrophotometrically at 350 nm versus time. A control sample with no oxo-anion added was prepared using the identical procedure described above except an equal volume of buffer was added in place of the phosphate analogue to prepare the control sample under the identical volume as the other samples. After the first addition of Fe^{2+} ions was monitored spectrophotometrically, the sample was removed from the spectrophotometer and stirred aerobically while 9 more additions of Fe^{2+} ions were added at 15 min intervals for a theoretical loading of 2000 Fe/ferritin. Another control was performed to determine the quantity of phosphate, arsenate, molybdate, or vanadate that bound to ferritin in the absence of added Fe^{2+} ions. Control samples were prepared identically to the above samples; only buffer was added in place of Fe^{2+} ions.

After the addition of iron and the indicated oxo-anion, the samples were centrifuged to remove any precipitated protein or small iron/oxo-anion complexes that may have formed during the incubation (complexes of Fe^{2+} and Fe^{3+} with the oxo-anions used are insoluble). The samples were then passed over a Sephadex G-25 column (1 × 20 cm) to separate any unbound iron or oxo-anions. A second, independent method to remove unbound ions was also employed. Unbound metals were removed using Amicon Ultra centrifugal filter devices with either a 30 000 or 100 000 molecular weight cutoff. The samples were concentrated to 200 μL and diluted with 5 mL 0.1 M Mops buffer pH 7.4 containing no iron or oxo-anions. The process of concentrating the protein to 200 μL and dilution was repeated 4 times to remove all unbound ions. Both methods used to remove unbound metals gave identical results. Protein concentrations were determined using the Lowry method.[32]

Elemental Analysis and UV/Vis Spectra. After unbound iron and oxo-anions were removed from the ferritin sample, the iron and oxo-anion concentrations of the samples were measured by inductively coupled plasma emission spectroscopy (ICP). The samples for ICP were prepared by removing an aliquot of each sample and denaturing the protein in 4% HNO_3. The ICP analysis was performed using the Perkin-Elmer Optima 3000 ICP spectrometer. Using the elemental analysis, the iron concentration of each sample was set at 0.25 mM Fe and the spectrum of each sample was recorded. Extinction coefficients were determined at 350 nm by taking the absorbance of each sample and dividing by the iron concentration of 0.25 mM Fe.

Iron Oxidation State and Mineral Release from Ferritin. The oxidation state of the iron in the new minerals was tested by treating the samples with α,α′-bipyridine to complex Fe^{2+} ion. Four aliquots were taken from each sample 15 min after the final addition of Fe^{2+} ions and reacted with α,α′-bipyridine. The first aliquot was analyzed spectrophotometrically, and the absorbance at 520 nm was

(15) Douglas, T.; Stark, V. T. *Inorg. Chem.* **2000**, *39*, 1828−1830.
(16) Yamashita, I. *Thin Solid Films* **2001**, *393*, 12−18.
(17) Allen, M.; Willits, D.; Young, M.; Douglas, T. *Inorg. Chem.* **2003**, *42*, 6300−6305.
(18) Meldrum, F. C.; Douglas, T.; Levi, S.; Arosio, P.; Mann, S. *J. Inorg. Biochem.* **1995**, *58*, 59−68.
(19) Douglas, T.; Dickson, D. P. E.; Betteridge, S.; Charnock, J.; Garner, C. D.; Mann, S. *Science* **1995**, *269*, 54−57.
(20) Wong, K. K. W.; Mann, S. *Adv. Mater.* **1996**, *8*, 928−931.
(21) Hainfeld, J. F. *Proc. Natl. Acad. Sci. U.S.A.* **1992**, *89*, 11064−11068.
(22) Meldrum, F. C.; Wade, V. J.; Nimmo, D. L.; Heywood, B. R.; Mann, S. *Nature* **1991**, *349*, 684−687.
(23) Warne, B.; Kasyutich, O. I.; Mayes, E. L.; Wiggins, J. A. L.; Wong, K. K. W. *IEEE Trans. Magn.* **2000**, *36*, 3009−3011.
(24) Hoinville, J.; Bewick, A.; Gleeson, D.; Jones, R.; Kasyutich, O.; Mayes, E.; Nartowski, A.; Warne, B.; Wiggins, J.; Wong, K. *J. Appl. Phys.* **2003**, *93*, 7187−7189.
(25) Mayes, E.; Bewick, A.; Gleeson, D.; Hoinville, J.; Jones, R.; Kasyutich, O.; Nartowski, A.; Warne, B.; Wiggins, J.; Wong, K. K. W. *IEEE Trans. Magn.* **2003**, *39*, 624−627.
(26) Okuda, M.; Iwahori, K.; Yamashita, I.; Yoshimura, H. *Biotechnol. Bioeng.* **2003**, *84*, 187−194.
(27) Scott, C. E.; Embaid, B. P.; Gonzalezjimenez, F.; Hubaut, R.; Grimblot, J. *J. Catal.* **1997**, *166*, 333−339.
(28) Centi, G.; Perathoner, S. *Top. Catal.* **2001**, *15*, 145−152.
(29) Ivanov, K.; Litcheva, P.; Krustev, S. *Oxid. Commun.* **2003**, *26*, 496−501.
(30) Abu-Shandi, K.; Winkler, H.; Wu, B.; Janiak, C. *CrystEngComm* **2003**, 180−189.
(31) Mehner, H.; Meisel, W.; Bruckner, A.; York, A. *Hyperfine Interact.* **1998**, *111*, 51−56.
(32) Lowry, O.; Rosenbrough, N.; Farr, A.; Randall, R. *J. Biol. Chem.* **1951**, *193*, 265−275.

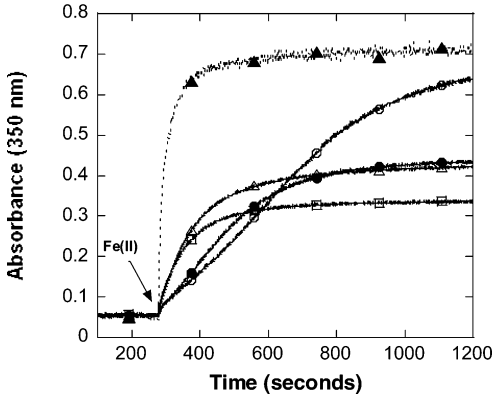

Figure 1. Change in absorbance at 350 nm was monitored vs time for a stirred solution of ferritin containing (○) no oxo-anion (iron-only control), (△) 1.0 mM phosphate, (□) 1.0 mM arsenate, (●) 1.0 mM molybdate, or (▲) 1.0 mM vanadate prepared in a spectrophotometer. The arrow indicates the addition of 200 Fe^{2+} ions/ferritin from a 0.01 M $FeSO_4$ stock solution.

used to detect the amount of Fe^{2+} ion present ($\epsilon_{520} = 8400\ M^{-1}\ cm^{-1}$). The other three aliquots were incubated for 1 h at 4, 23, and 37 °C to determine if Fe^{2+} ion release from the new mineral was slow or temperature dependent. After 1 h the samples were read at 520 nm to determine the amount of Fe^{2+} ion released. Finally, the samples were treated with dithionite to reduce the iron in the mineral core so the complete iron content could be analyzed.

Electron Microscopy. Transmission electron microscopy samples were prepared on SPI holey carbon coated Cu grids and were imaged using a JEOL-Jem 2010 electron microscope at 40, 50, and 120 keV using an Oxford ISIS energy-dispersive X-ray analysis system. Samples were prepared by applying an aqueous ferritin solution onto a 200-mesh carbon-coated Cu TEM grid followed by air-drying the sample.

Results

Iron Incorporation. The kinetics of iron incorporation into ferritin has been studied previously using spectrophotometric methods by monitoring the absorbance change at several wavelengths between 310 and 420 nm.[33−39] This change in absorbance has been attributed to the formation of the Fe(III) oxide hydroxide mineral core in ferritin. Using these established methods, the incorporation of iron into ferritin was monitored in the absence and presence of the indicated oxo-anions.

Figure 1 shows data for the addition of 200 Fe^{2+} ions/apo-ferritin in the presence and absence of various oxo-anions. Several interesting differences are observed between the kinetic curves. The first difference is that the initial rate of iron binding and oxidation is slowest in the control sample containing no oxo-anions. The sample prepared in the absence of a phosphate analogue has a sigmoidal curve. The sigmoidal progression of iron loading into ferritin has been observed previously[35] and an explanation for this observed behavior proposed by ref 40. The presence of an oxo-anion produces a faster initial rate in each case and changes the shape of the curve from sigmoidal to hyperbolic (Figure 1). Further analysis of Figure 1 shows that the final absorbance of the various samples is different from the iron-only control although 200 Fe^{2+} ions/ferritin were added to each instance. Data in Table 1 indicate that the different final absorbance in each sample is due to the formation of different iron oxo-anion minerals in ferritin that possess different extinction coefficients.

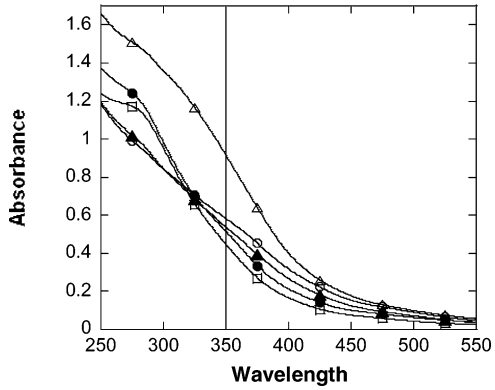

Figure 2. Spectra of ferritin samples loaded with 2000 iron atoms/ferritin with (○) no oxo-anion present (iron-only control), (▲) 1.0 mM phosphate, (□) 1.0 mM arsenate, (●) 1.0 mM molybdate, or (△) 1.0 mM vanadate. Unbound ions were separated from ferritin by gel filtration chromatography. The samples were adjusted to the same iron concentration (0.25 mM), and the spectrum of each sample was recorded on an Agilent 8453 diode array spectrophotometer. The line at 350 nm indicates the wavelength used to monitor iron loading in Figure 1.

Table 1. Elemental Analysis of Ferritin Samples[a]

sample	Fe/HoSF	anion/HoSF	Fe/oxo-anion	ϵ_{350nm}
apo-HoSF + PO_4^{3-}	6 ± 1	11 ± 1	NA	NA
apo-HoSF + AsO_4^{3-}	5 ± 1	23 ± 4	NA	NA
apo-HoSF + VO_4^{3-}	4 ± 2	ND	NA	NA
apo-HoSF + MoO_2^{2-}	6 ± 1	16 ± 1	NA	NA
apo-HoSF + Fe^{2+} ions	2098 ± 17	ND	NA	2325
apo-HoSF + PO_4^{3-} + Fe^{2+}	1491 ± 160	319 ± 14	4.7:1	1783
apo-HoSF + AsO_4^{3-} + Fe^{2+}	1697 ± 103	761 ± 47	2.2:1	2053
apo-HoSF + VO_4^{3} + Fe^{2+}	1685 ± 156	2255 ± 74	1:1.3	3659
apo-HoSF + MoO_2^{2} + Fe^{2+}	1934 ± 41	1261 ± 90	1.5:1	2148

[a] Samples were prepared as described in the Experimental Section. The ϵ_{350nm} values were calculated by preparing all samples at 0.25 mM Fe and recording the absorbance at 350 nm. The abbreviations are as follows: HoSF, horse spleen ferritin; ND, not detected; NA, not applicable.

After the samples shown in Figure 1 were treated with 9 more additions of iron, the unbound ions were separated from the protein by gel-filtration chromatography or centrifugal filter separation techniques, and elemental analysis was performed to determine the extent of iron and oxo-anion loading into ferritin samples. Significant quantities of oxo-anions were associated with the ferritin cores (Table 1). An interesting observation is that all of the oxo-anions studied were incorporated into ferritin at higher ratios than the native phosphate. Molybdate and arsenate were incorporated into ferritin at approximately 2 Fe/oxo-anion, whereas vanadate was found at a higher ratio than iron (1 Fe/1.3 V). Control

(33) Macara, I. G.; Hoy, T. G.; Harrison, P. M. *Biochem. J.* **1972**, *126*, 151−162.
(34) Macara, I. G.; Hoy, T. G.; Harrison, P. M. *Biochem. J.* **1973**, *135*, 343−348.
(35) Paques, E. P.; Paques, A.; Crichton, R. R. *J. Mol. Catal.* **1979**, *5*, 363−375.
(36) Paques, E. P.; Paques, A.; Crichton, R. R. *Eur. J. Biochem.* **1980**, *107*, 447−453.
(37) Levi, S.; Luzzago, A.; Cesareni, G.; Cozzi, A.; Franceschinelli, F.; Albertini, A.; Arosio, P. *J. Biol. Chem.* **1988**, *263*, 18086−18092.
(38) Orino, K.; Kamura, S.; Natsuhori, M.; Yamamoto, S.; Watanabe, K. *Biometals* **2002**, *15*, 59−63.
(39) Aitken-Rogers, H.; Singleton, C.; Lewin, A.; Taylor-Gee, A.; Moore, G. R.; Le Brun, N. E. *J. Biol. Inorg. Chem.* **2004**, *9*, 161−170.

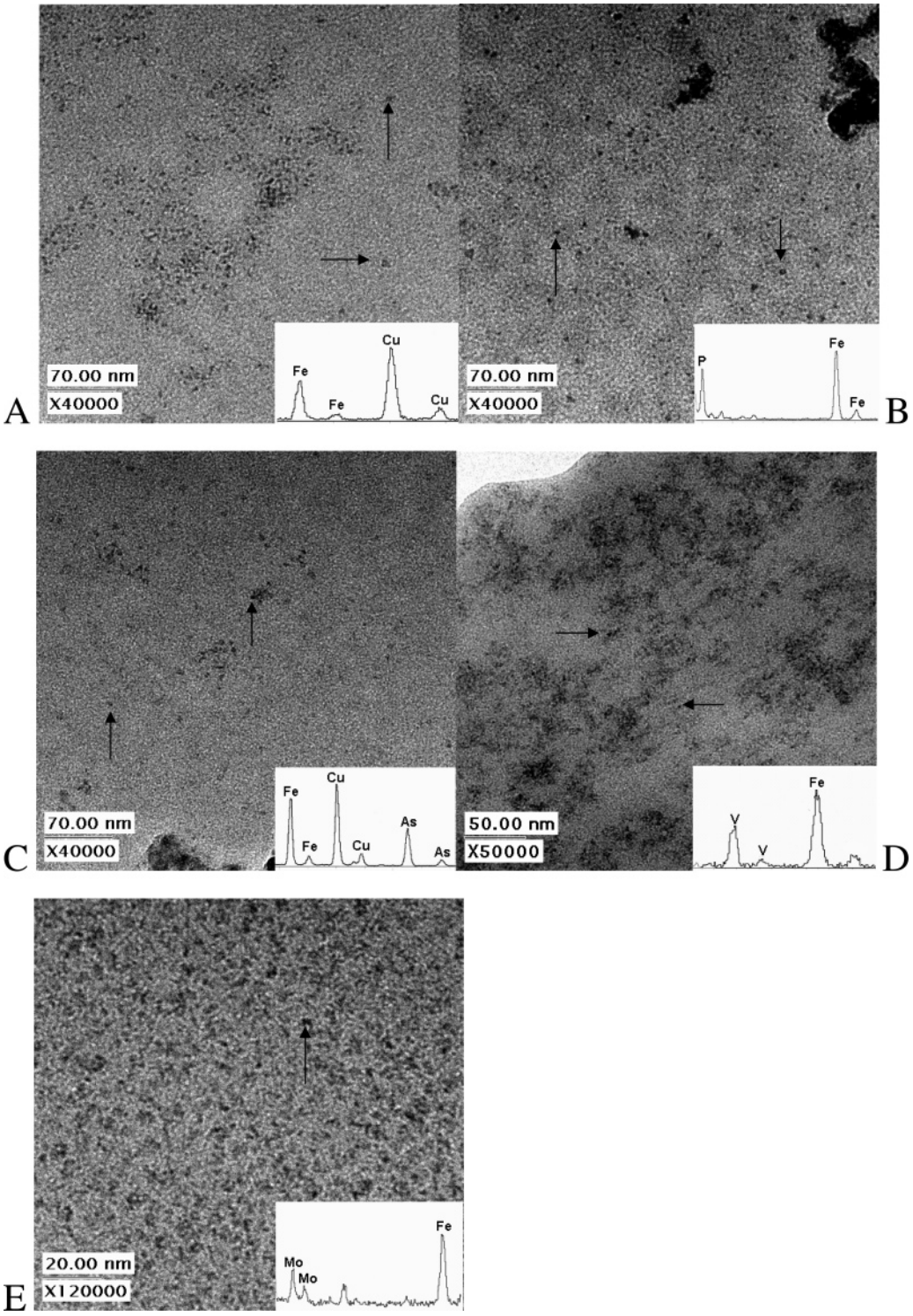

Figure 3. Transmission electron micrographs of ferritin containing (A) only iron (40 keV), (B) iron and phosphate (40 keV), (C) iron and arsenate (120 keV), (D) iron and vanadate (40 keV), and (E) iron and molybdate (50 keV). The inset in each sample shows the energy-dispersive X-ray analysis (edxa) data indicating the presence of iron and the appropriate element for the indicated oxo-anion; Cu is also shown in the edxa data due to the Cu sample holder.

experiments indicate that less than 24 oxo-anions (~1/subunit) bind to apo-ferritin in the absence of added iron, showing that the incorporation of oxo-anion requires both iron and oxo-anion. This observation is consistent with the observations for phosphate binding to apo-bacterial ferritin where only 6 phosphate ions were reported to bind to apo-bacterial ferritin.[39] Table 1 also shows the extinction coefficients for the oxo-anion-containing samples at 350 nm.

Electron Microscopy. Transmission electron microscopy was used to evaluate the loading of the iron and oxo-anions and to confirm that the minerals formed inside the ferritin interior (Figure 3). Analysis of ferritin loaded with each of the oxo-anions (Figure 3B−E) revealed electron dense mineral cores consistent with the ~8 nm interior of ferritin and comparable to the sample loaded with iron in the absence of oxo-anions (Figure 3A). Ferritin samples containing oxo-

anions in the mineral cores showed no electron diffraction from these cores suggesting that the material was amorphous. This result is consistent with previous observations for ferritin samples containing high phosphate content.[8,10,41] Energy-dispersive X-ray analysis of the cores provided a qualitative comparison to the ICP data indicating the presence of iron and the oxo-anion loaded at similar ratios observed in Table 1. The presence of Cu from the TEM grids was also observed. TEM data establish that the iron and the oxo-anions are sequestered inside ferritin and form cores similar to that of native ferritin.

UV/Vis Spectra. The samples shown in Table 1 were prepared at an iron concentration of 0.25 mM, and the spectrum of each sample was recorded. The results are shown in Figure 2. As expected from Figure 1, the sample containing only iron has a higher absorbance at 350 nm than the samples containing phosphate, arsenate, and molybdate. Note that the samples here were loaded with ~2000 Fe/ferritin in the presence of 1.0 mM concentrations of the indicated oxo-anions. The data in Figure 1 are the rate of iron loading during the first addition of the 10 additions that produced the sample analyzed in Figure 2. The sample containing vanadate has the highest absorbance through the range from 250 to 550 nm. Since each sample contains the same iron concentration, the extinction coefficient for the absorbance of the iron oxo-anion complex of each sample could be determined at 350 nm, and the results are shown in Table 1. Since the extinction coefficients are different for each iron oxo-anion complex, we conclude that a different iron oxo-anion mineral forms in each ferritin sample.

Mineral Release from Ferritin. After the preparation of a new mineral core containing 1000 Fe/ferritin in the presence of phosphate, arsenate, vanadate, or molybdate, the samples were treated with α,α′-bipyridyl to determine the oxidation state of the iron. The addition of α,α′-bipyridyl 15 min after the last addition of iron did not produce the $Fe(bipy)_3^{2+}$ complex (observed at 520 nm). This observation indicates that no Fe^{2+} ions were present in solution. Furthermore, it indicates that no Fe^{2+} ions were available to be chelated from the interior of ferritin. Each sample was incubated at 4, 25, or 37 °C for 1 h and measured again for the formation of the $Fe(bipy)_3^{2+}$ complex. No increase in the $Fe(bipy)_3^{2+}$ complex was observed after this treatment. Finally, sodium dithionite was added to chemically reduce the iron in the mineral core and the $Fe(bipy)_3^{2+}$ complex formed rapidly. These studies indicate that the oxidation state of the iron in each of the oxo-anion complexes was Fe(III). The concentration of iron matched the total iron added and confirms that all of the iron was released from ferritin by dithionite and bipyridyl treatment.

Discussion

The results presented are consistent with the interpretation that phosphate and the analogues of phosphate used in this study stimulate the rate of iron loading into ferritin and become incorporated into the resulting mineral core. These results have implications toward many aspects of ferritin research. Since phosphate occurs naturally in cells, the observation that phosphate stimulates the rate of iron loading into ferritin may be physiologically relevant to properly understand the iron loading process in vivo. Furthermore, V and Mo have biological roles as catalysts in the active sites of some enzymes[42−44] and the incorporation of anions of these metals into ferritin indicates the possibility that these metals may be stored in ferritin in vivo. Finally, the 8 nm interior diameter of ferritin has previously been used as a constrained reaction environment for the synthesis of nanomaterials. The use of oxo-anions may provide a new synthetic route to prepare nanomaterials in the core of ferritin. These issues will be discussed in the context of the results presented above.

In Figure 1, the iron loading curves suggest that the oxo-anions stimulate the rate of iron loading into ferritin. The loading in the presence of oxo-anions produces a hyperbolic kinetic curve compared to the sigmoidal curve in the control without oxo-anions. The sigmoidal shape of the curve can be explained using a two-step model for iron loading. The early, slower section of the curve has been attributed to iron oxidation at the ferroxidase center.[40] The effect of iron binding and oxidation at the ferroxidase site occurs with less than 50 Fe/ferritin.[40] As the mineral core begins to form, iron oxidation begins to occur at the mineral core surface.[35,40] The observed behavior is understandable if the oxidation of iron on the mineral core surface is faster than the oxidation occurring at the ferroxidase center. Therefore, the sigmoidal curve for the iron only sample is the expected result for 200 Fe^{2+} ions added/ferritin. The presence of oxo-anions apparently alters this mechanism. Several factors could be involved in this change in the iron loading process. Cheng et al. proposed that phosphate could bind at the ferroxidase site and shift the redox potential to a more negative value increasing the rate of iron oxidation.[45] Similarly, Aitken-Rogers et al. suggested that phosphate may bridge the iron atoms bound at the ferroxidase site but proposed that the most likely mechanism was probably a remote interaction near the ferroxidase site.[39] Cheng et al. further identified a role for phosphate in stimulating the rate of iron migration from the ferroxidase site to the interior of the ferritin.[45] Huang et al. and Johnson et al. demonstrated that phosphate promotes iron binding to the mineral core surface and causes a stimulation in the rate of oxidation of the Fe^{2+} ion bound on mineral core surface.[13,46] It is possible that the presence of oxo-anions during the nascent formation of the mineral core allows the surface oxidation reaction to occur at a much lower iron loading than in the absence of oxo-anions. If this is the case, the observed stimulation of the rate of iron

(40) Sun, S.; Chasteen, N. D. *J. Biol. Chem.* **1992**, *267*, 25160−25166.
(41) Mann, S.; Williams, J. M.; Treffry, A.; Harrison, P. M. *J. Mol. Biol.* **1987**, *198*, 405−416.
(42) Slebodnick, C.; Hamstra, B. J.; Pecoraro, V. L. *Met. Sites Proteins Models* **1997**, *89*, 51−108.
(43) Chasteen, N. D. *Met. Ions Biol. Syst.* **1995**, *31*, 231−47.
(44) Hille, R. *Chem. Rev.* **1996**, *96*, 2757−2816.
(45) Cheng, Y. G.; Chasteen, N. D. *Biochemistry* **1991**, *30*, 2947−2953.
(46) Johnson, J. L.; Cannon, M.; Watt, R. K.; Frankel, R. B.; Watt, G. D. *Biochemistry* **1999**, *38*, 6706−6713.

incorporation into ferritin may be a combined effect of the oxo-anions stimulating the rate of iron transport across the protein shell into the interior of ferritin followed by a stimulated rate of iron oxidation on the mineral core surface. This suggests that a small iron phosphate (or iron oxo-anion) complex located at the nucleation site at the interior of ferritin will bind and oxidize Fe^{2+} earlier in the mineralization process than an iron mineral lacking an oxo-anion. Further experiments are required to provide more mechanistic information regarding the iron loading process in the presence of oxo-anions. It is interesting to note that Paques et al. reported a hyperbolic iron-loading curve when performing iron incorporation experiments using the buffer dimethyl arsenate, an analogue of arsenate used in this study.[35]

Many factors may influence the formation of these new iron/oxo-anion mineral cores. These include oxo-anions size, charge, geometry, and protonation state. Each of these anions is tetrahedral in geometry with the exception of certain species of V and Mo, which may exist as polymers (see below). The size increases with the ionic radius of each anion as follows: $PO_4^{3-} = 210$ pm, $AsO_4^{3-} = 234$ pm, $VO_4^{3-} = 258$ pm, and $MoO_4^{2-} = 264$ pm (calculated from Pauling ionic radius tables). Crystallographic analysis of the 4-fold channel of ferritin suggest that a 200 pm diameter molecule could diffuse through this channel making these anions slightly too large for entry through this pore.[47] Similar calculations can be made for diffusion through the 3-fold channel since Ca^{2+} was observed in the crystal structure and is coordinated by 6 oxygen ligands from carboxylate groups. With a Pauling ionic radius of 99 pm, the diameter of Ca^{2+} is 198 pm indicating that this channel is also too small to accommodate the oxo-anions without invoking a breathing motion to allow these anions to pass through the channel. Since the largest anion, molybdate, was incorporated at a higher ratio than the smallest anion, phosphate, we postulate that the increased anion size does not have sufficient steric effects to be inhibitory toward the normal mechanism of anion entry into ferritin.

The mechanism for anions entering the interior of ferritin is difficult to understand. Molecular diffusion experiments of small nitroxide spin probe radicals (7−9 Å) showed that positively charged species entered the ferritin core but negatively charged species did not enter ferritin.[48] Calculations of electrostatic gradients of the ferritin protein surface show that the 3-fold channels are negatively charged and promote the entry of cations but the large negative potentials at the 3-fold and 4-fold channels should repel the oxo-anions.[3] Additional electrostatic gradient calculations and examination of alternate entry sites are underway to determine how anions enter and leave the interior of ferritin.

The speciation state of each anion in solution is another property that may affect iron loading into ferritin. At pH 7.4 the predominant protonation state of the phosphate and arsenate anions will be ~70% HPO_4^{2-} and $HAsO_4^{2-}$ ions with the other species $H_2PO_4^-$ and $H_2AsO_4^-$ present at about 30%. Vanadate will exist as $H_2VO_4^-$ or may form VO_3^-. It is possible that changing the shape and charge and protonation state to VO_3^- could significantly increase the rate of iron incorporation into ferritin. Control experiments with the analogue NO_3^- (data not shown) showed no change in iron incorporation into ferritin compared to the iron only control suggesting that the VO_3^- species was not responsible for the increased rate of vanadate loading into ferritin (data not shown). At higher concentrations vanadate may exist as $V_3O_9^{3-}$ or $V_4O_{12}^{4-}$[49] and molybdate polymers ($Mo_2O_7^{2-}$) also exist at intermediate pH.[50] It is assumed that the larger size of polymers would have difficulty passing through the channels of ferritin and are not further considered. The effect of charge may alter the effectiveness of incorporating the anions into ferritin. Assuming the major species at pH 7.4 are HPO_4^{2-}, $HAsO_4^{2-}$, and $H_2VO_4^-$ or VO_3^-, a slight deficit in charge is found for vanadate. Molybdate as MoO_4^{2-} has charge similar to those of HPO_4^{2-} and $HAsO_4^{2-}$ but has a different protonation state. The data in Table 1 show no obvious trend for the effect of charge of the anions used.

Figure 1, Figure 2, and Table 1 all show that the presence of the oxo-anions alter the absorbance properties of the resulting mineral formed in ferritin. One explanation for the lower final absorbance of the phosphate, arsenate, and molybdate samples in Figure 1 is that some of the added Fe^{2+} ions could have precipitated in solution by forming insoluble iron oxo-anion complexes. Fe^{2+} and Fe^{3+} oxo-anion complexes are quite insoluble ($Fe_2(PO_4)_2$ $K_{sp} = 1 \times 10^{-36}$, $FePO_4$ $K_{sp} = 4.0 \times 10^{-27}$, $Fe_3(AsO_4)_2$ $K_{sp} = 1.8 \times 10^{-41}$, $FeAsO_4$ $K_{sp} = 1.26 \times 10^{-21}$, $Fe(VO_3)_2$ $K_{sp} = 1.6 \times 10^{-18}$, $FeMoO_4$ $K_{sp} = 1.7 \times 10^{-9}$).[51,52] The elemental analysis shows that the phosphate, arsenate, vanadate, and molybdate samples loaded 71%, 80%, 80%, and 92% of the theoretical loading of the iron only sample. Although these data suggest that a portion of the iron did precipitate under these experimental conditions, they also demonstrate the remarkable iron sequestering ability of ferritin to internalize a 200-fold excess of iron in a 1.0 mM oxo-anion solution considering the solubility product data reported above. In fact, control experiments without ferritin form insoluble precipitates immediately upon the addition of iron to the solutions, demonstrating the ability of ferritin to direct added iron into its interior despite the competing low solubility of nonspecific iron/oxo-anion mineral formation reactions. The altered absorbance properties of ferritin were confirmed by preparing the samples at a constant iron concentration and demonstrating that a new iron/oxo-anion mineral is formed in the presence of each oxo-anion and that these new mineral phases each have a different extinction coefficient. Decreased

(47) Hempstead, P. D.; Yewdall, S. J.; Fernie, A. R.; Lawson, D. M.; Artymiuk, P. J.; Rice, D. W.; Ford, G. C.; Harrison, P. M. *J. Mol. Biol.* **1997**, *268*, 424−448.
(48) Yang, X.; Arosio, P.; Chasteen, N. D. *Biophys. J.* **2000**, *78*, 2049−59.
(49) Pope, M. T.; Muller, A. *Heteropoly and Isopoly Oxometalates*; Springer-Verlag: Berlin, 1983; p 180.
(50) Day, V. W.; Fredrich, M. F.; Klemperer, W. G.; Shum, W. *J. Am. Chem. Soc.* **1977**, *99*, 6146−6148.
(51) Martell, A. E.; Smith, R. M. *Critical Stability Constants*; Plenum Preses: New York, 1976; Vol. 4.
(52) Lide, D. R. *CRC Handbook of Chemistry and Physics*, 77th ed.; CRC Press: New York, 1996; pp 8−90.

extinction coefficients have been reported for iron cores prepared in the presence of phosphate during iron loading experiments.[5,39]

The electron micrograph (EM) data confirm that the iron oxo-anion complexs form discrete mineral particles of a size consistent with the interior dimensions of ferritin suggesting that the mineral is sequestered inside the protein shell of ferritin. This interpretation could be inferred from the elemental analysis data due to the extremely large number of ions associated with the ferritin, but the EM data confirm this interpretation of the data. The cores formed with the phosphate analogues all lacked electron diffraction properties indicating that they are similar in nature to the amorphous iron phosphate cores previously studied.[8,10,41]

The incorporation of molybdate and vanadate into ferritin is interesting because each of these metals has biological function at the active sites of enzymes.[42−44] Furthermore, vanadium has been reported to be a native component of horse spleen ferritin at levels of 5−10 V/ferritin.[53] Analysis of native holo-horse spleen ferritin samples (containing ~1500 Fe/ferritin) obtained directly from Sigma showed that 20 atoms of V and 10 atoms of Mo were present. We propose that ferritin may act as a storage site for these metals in biological systems as well as for iron.

The incorporation of Mo and V into ferritin in the presence of iron also introduces the concept of co-incorporating multiple transition metal ions into ferritin for materials synthesis applications. Ferritin samples have been prepared containing many interesting nonnative metal cores such as Co,[15] Mn,[18] CdS,[20] FeS,[19] CoPt,[23] and U.[21,22] The comineralization of metal ions with phosphate analogues may present a new and novel synthetic route to preparing protein-encapsulated nanomaterials with new and interesting properties.

Conclusions

The data presented demonstrate that the oxo-anions arsenate, molybdate, and vanadate are sequestered along with iron inside the protein shell of ferritin in a fashion similar to that of the native phosphate anion. The incorporation of these anions resulted in an increased rate of iron oxidation as well as an altered final absorbance of the resulting mineral cores (Figure 1). Elemental analysis confirms that large quantities of iron and the oxo-anions migrate with the ferritin protein through gel filtration chromatography suggesting that the mineral phase is sequestered inside the ferritin protein shell. TEM results confirm that an amorphous mineral phase is present in discrete 8 nm particles consistent with the formation of iron mineral cores inside the 8 nm interior of the ferritin protein. Taken together, these data demonstrate that the oxo-anions arsenate, vanadate, and molybdate are readily incorporated into ferritin during iron loading in the same manner as the native phosphate anion.

Acknowledgment. We thank the University of New Mexico Department of Chemistry for funding this research project.

IC048819R

(53) Grady, J. K.; Shao, J. L.; Arosio, P.; Santambrogio, P.; Chasteen, N. D. *J. Inorg. Biochem.* **2000**, *80*, 107−113.